Experimental observation of the effect of global phase on optimal times of SU(2) quantum operations

Ji Bian,[1,2] Xi Chen,[1,2] Ran Liu,[1,2] Zhennan Zhu,[1,2] Xiaodong Yang,[1,2] Hui Zhou,[3,*] and Xinhua Peng[1,2,4,†]

[1]*Hefei National Laboratory for Physical Sciences at the Microscale and Department of Modern Physics, University of Science and Technology of China, Hefei 230026, China*

[2]*CAS Key Laboratory of Microscale Magnetic Resonance, University of Science and Technology of China, Hefei, Anhui 230026, China*

[3]*Department of Physics, Shaanxi University of Science and Technology, Xi'an 710021, China*

[4]*Synergetic Innovation Center of Quantum Information and Quantum Physics, University of Science and Technology of China, Hefei, Anhui 230026, China*

(Received 30 June 2019; published 16 October 2019)

We study the role that the global phase plays in quantum operations. Previous theoretical works suggested that the optimal (minimum) times to realize SU(n) quantum operations with different global phases are generally different. Here, we experimentally constructed two SU(2) operations with different global phases, i.e., U and $-U$, in optimal times. Then, utilizing nuclear magnetic resonance interferometry, we measured these phases and observed the global phase's effect on the optimal times of these two operations. Our result further clarifies that the effect that the global phase has on unitary operations is not only mathematical, but also physical. In addition, this work has potential applications in many areas, such as designing time-optimal controls in quantum systems.

DOI: 10.1103/PhysRevA.100.042315

I. INTRODUCTION

The global phase in quantum mechanics has been studied from various aspects, e.g., Refs. [1–7], to name a few. While most of these works have focused on the global phase of quantum states, little attention has been paid to its role in evolution operators. For example, given two operations in SU(n) that only differ from each other by a global phase, one may ask if, apart from their difference in mathematical format, there is any physical difference between them. The answer is yes and, for example, one well-known effect resulting from this difference is the overall phase change acquired after the 2π rotation of a particle [6,8]. This distinguishes fermions from bosons [4], which has been observed in experiments via interferometric approaches [9,10].

Recently, several theoretical works have drawn a clear distinction among operations with different global phases [11–16] from a different angle. They show that the minimum (optimal) times to realize such operations is, in general, different. Reference [12] theoretically explores the relation between the global phase of a SU(2) operation and the corresponding optimal time to realize such an operation. In addition, the relation between the global phase and the optimal time of SU(3) operations, e.g., quantum Fourier transform gate, was also given under the assumption of unbounded control strength [14,15]. These theoretical works help one to upgrade the role of the global phase in unitary operations from a pure mathematical one to a physical one. However, there is no experimental demonstration that relates the theoretical constructs to an observable phenomenon.

In this paper, we propose a general scheme to detect the global phase of unitary operations in SU(2), and explore its effect on the optimal time to realize such operations via the nuclear magnetic resonance (NMR) technique. Our experiment, combined with those theoretical works [12–18], help to clarify the effect that the global phase has on unitary operations. Keeping this effect in mind has practical impacts. For example, it helps to design quantum gates with smaller durations in quantum information science. It also helps to achieve a better pulse optimization procedure in magnetic resonance spectroscopy [17,18].

This paper is organized as follows. In Sec. II, we first present the possible global phases of a SU(n) operation. Then we briefly review the result of time-optimal control (TOC) for SU(2) operations given in [12]. In Sec. III, we propose the scheme to construct two SU(2) operations with different global phases in optimal times, and detect their global phases via interferometric approaches. Section IV provides a proof-of-principle experiment with a two-qubit NMR quantum processor. Some discussions are also given in this section. The conclusion is given in Sec. V.

II. TIME-OPTIMAL CONTROL AND GLOBAL PHASE OF UNITARY OPERATIONS

For a typical closed quantum system (with dimension n), we assume the unitary operation $U \in \mathrm{SU}(n)$. The question is as follows: if we multiply U by a phase factor $e^{i\phi}$, $\phi \in [0, 2\pi)$, will the result still belong to SU(n)? The answer is as follows: only when the phase ϕ takes some discrete values [13], which can be seen from the following proof.

Proof. Let the operation $U_a \in \mathrm{SU}(n)$ and $U_b = e^{i\phi}U_a$. If $U_b \in \mathrm{SU}(n)$, then we have

$$P := U_b U_a^{-1} \in \mathrm{SU}(n). \tag{1}$$

*zhouhui9240@163.com
†xhpeng@ustc.edu.cn

Note that $\mathrm{Det}(P) = e^{in\phi} = 1$; then, ϕ can only take some discrete values, i.e.,

$$\phi = 0, \frac{2\pi}{n}, \ldots, \frac{2(n-1)\pi}{n}. \tag{2}$$

■

The above result tells us that given a unitary operation, what all the other operations with a global phase difference are. For example, for $U_{a,b} \in \mathrm{SU}(2)$, the allowable phases are $\phi = 0, \pi$, while for $U_{a,b} \in \mathrm{SU}(3)$, $\phi = 0, 2\pi/3, 4\pi/3$. In the following, we would choose a fixed reference operation and define the *global phase* of a unitary operation U relative to this reference. For example, if U_a is chosen to be the reference, then we say the global phase of $U_b = e^{i\phi}U_a$ is ϕ.

Consider the time-optimal control problem in a single-qubit closed system. The Hamiltonian of the system here reads

$$H_a = -\omega_x(t)I_x - \omega_y(t)I_y - \omega I_z, \tag{3}$$

where the operators

$$I_x = \frac{1}{2}\begin{pmatrix} 0 & 1 \\ 1 & 0 \end{pmatrix}, \quad I_y = \frac{1}{2}\begin{pmatrix} 0 & -i \\ i & 0 \end{pmatrix}, \quad I_z = \frac{1}{2}\begin{pmatrix} 1 & 0 \\ 0 & -1 \end{pmatrix},$$

in the unit of $\hbar = 1$, $\omega_{x,y}$ are control fields with a constant upper bound, i.e., $\omega_x^2 + \omega_y^2 \leqslant \omega_{\max}^2$, and ω is the detuning. The TOC in this scenario has been well studied theoretically by Garon *et al.* [12]. There geometric principles are used to obtain the TOC for both the on-resonance case ($\omega = 0$) and the off-resonance case ($\omega \neq 0$). The equations for the TOC along arbitrary axes are given. Moreover, a thorough analysis of the difference between the optimal times of SU(2) operations U and $-U$ is presented. Note from (2) that this has already covered all the possible global phases one can add upon U.

Base on their result, here we pay close attention to the on-resonance ($\omega = 0$) case, where the desired TOC rotation axes $\vec{n}_0$ lie in the $x-y$ plane. Denote $R_{\vec{n}}(\theta) := e^{-i\vec{n}\cdot\vec{I}\theta}$, where $\vec{n}$ is a unit vector, $\vec{I} = (I_x, I_y, I_z)$, and θ is the rotation angle [note here that $R_{\vec{n}}(\theta)$ only denotes a unitary operation belongs to SU(2), not any particular control method]. According to [12], the optimal time T_+ for $R_{\vec{n}_0}(\theta)$ and T_- for $-R_{\vec{n}_0}(\theta)$, with $\theta \in [0, 4\pi)$, satisfies the following relation:

$$\begin{aligned} &T^+ < T^-, && 0 \leqslant \theta < \pi, \\ &T^+ = T^-, && \theta = \pi, \\ &T^+ > T^-, && \pi < \theta < 3\pi, \\ &T^+ = T^-, && \theta = 3\pi, \\ &T^+ < T^-, && 3\pi < \theta < 4\pi. \end{aligned} \tag{4}$$

This fact is somewhat surprising [13] since we normally take any U and $-U$ to be the same operation (this is due to the two-to-one homomorphic mapping of SU(2) onto SO(3) [19]). Such relations draw a clear distinction among unitary operations with different global phases. However, to our best knowledge, there is a lacking of experimental demonstration.

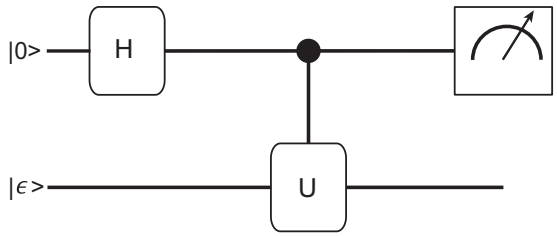

FIG. 1. Quantum circuit for detecting the global phases of different unitary operations.

III. GLOBAL PHASE DETECTION VIA INTERFEROMETRY SCHEME

Without loss of generality, here we choose $\theta = \pi/2$, $\vec{n}_0$ along the y axis, and $\pm U_{\mathrm{id}}$ denotes the target operations realized in minimum time for the system (3), which corresponds to the first case in Eqs. (4). According to [12], the corresponding TOC for $\pm U_{\mathrm{id}}$ is just a constant control field added in $\pm y$ axes with maximum control strength $\omega_{\max}$, and different durations,

$$T^+ = \frac{\pi}{2\omega_{\max}}, \quad T^- = \frac{3\pi}{2\omega_{\max}}, \tag{5}$$

which is a clear indication that the duration of the two operations is different and satisfies the relation $T^+/T^- = 1/3$. In the following, $+U_{\mathrm{id}}$ is chosen as the reference (with global phase 0), and the goal is to detect the global phase of $-U_{\mathrm{id}} = e^{i\pi}U_{\mathrm{id}}$, i.e., $\phi = \pi$.

Global phase detection can be realized via interferometric approaches, e.g., optical interferometry [5,20], neutron interferometry [9,21], and NMR interferometry [7,22]. The main idea is to introduce an ancilla qubit (qubit 1) which is coupled to the system (qubit 2) and encode the global phase of the operation to the relative phase of the whole system, then read out the encoded information through the ancilla qubit. The interferometric scheme (Fig. 1) is implemented via the following procedure:

(1) Prepare the superposition state of the ancilla with the Hadamard gate H; then, the whole system becomes

$$|\psi_a\rangle = \frac{1}{\sqrt{2}}(|0\rangle + |1\rangle) \otimes |\epsilon\rangle, \tag{6}$$

where the system is in an arbitrary state $|\epsilon\rangle = \epsilon_0|0\rangle + \epsilon_1|1\rangle$, $I_z|0\rangle = \frac{1}{2}|0\rangle$, $I_z|1\rangle = -\frac{1}{2}|1\rangle$, and $\epsilon_{0,1}$ are complex coefficients satisfying $|\epsilon_0|^2 + |\epsilon_1|^2 = 1$.

(2) Construct $\pm U_{\mathrm{id}}$ on the system and encode the global phases of the two operations through applying the controlled operation

$$C_{\pm U_{\mathrm{id}}} = e^{-i\alpha^{\pm}(|1\rangle\langle 1|\otimes I_{2y})} = e^{-i(|1\rangle\langle 1|\otimes H_{\mathrm{id}}^{\pm})T^{\pm}}, \tag{7}$$

where $\alpha^+ = \pi/2$, $\alpha^- = -3\pi/2$, and the operator $H_{\mathrm{id}}^{\pm} = \pm\omega_{\max}I_{2y}$ is the TOC control Hamiltonian. Note that different qubits are labeled by different numbers in the subscript. Then the state becomes

$$|\psi_b^{\pm}\rangle := \frac{1}{\sqrt{2}}(|0\rangle \otimes |\epsilon\rangle + |1\rangle \otimes |\lambda^{\pm}\rangle), \tag{8}$$

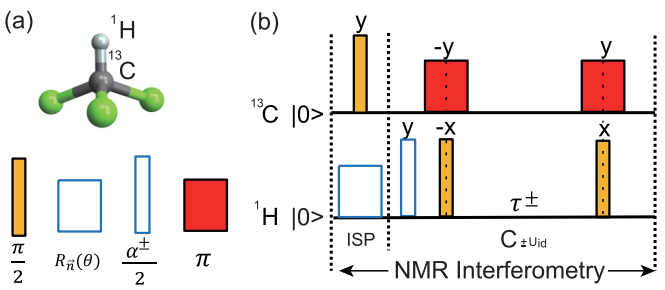

FIG. 2. (a) The molecular structure of the chloroform sample. (b) Pulse sequence in NMR experiments. Note that the $R_{\vec{n}}(\theta)$ pulse (on ^{1}H) is applied to create $|\epsilon\rangle$, $R_{1y}(\pm\pi)$ pulses (on ^{13}C) are only applied for $C_{-U_{\rm id}}$. $\alpha^{\pm}$ and $\tau^{\pm}$ are given in the main text.

where the state $|\lambda^{\pm}\rangle := \pm\frac{1}{\sqrt{2}}[(\epsilon_0-\epsilon_1)|0\rangle+(\epsilon_0+\epsilon_1)|1\rangle]$. From (7) and (8), we can see that the desired TOC operation (on qubit 2) is realized by the above controlled operation when the first qubit is in $|1\rangle$. The final state can be expanded and reads

$$|\psi_b^{\pm}\rangle = \frac{1}{\sqrt{2}}\Big[\epsilon_0|00\rangle+\epsilon_1|01\rangle \pm \frac{1}{\sqrt{2}}(\epsilon_0-\epsilon_1)|10\rangle \pm \frac{1}{\sqrt{2}}(\epsilon_0+\epsilon_1)|11\rangle\Big], \tag{9}$$

and the global phases of $\pm U_{\rm id}$ are now encoded in the relative phases of the whole system.

(3) Read out the relative phases (with the global phase ϕ encoded in) directly or convert them to populations (then read out) [23], depending on the experimental apparatus.

IV. EXPERIMENT

The experiment is carried out on a Bruker Avance III 400 MHz (9.4 T) spectrometer at room temperature. We use the ^{13}C-labeled chloroform dissolved in d_6 acetone as a two-qubit NMR quantum processor, where the ^{13}C nucleus is used for the ancilla qubit (qubit 1) while ^{1}H is used for the system qubit (qubit 2). The molecular structure is shown in Fig. 2(a). The natural Hamiltonian of this two-qubit system in a double-resonance rotating frame is given by

$$H_{\rm nmr} = 2\pi J I_{1z}I_{2z}, \tag{10}$$

where the coupling constant J is 214.5 Hz and the relaxation times T_2 are 0.3 s and 2.8 s for ^{13}C and ^{1}H, respectively.

The experiment consists of the following steps: (1) initial-state preparation (ISP), (2) the controlled operation, and (3) measurement. The NMR pulse sequence corresponding to the quantum circuit in Fig. 1 is illustrated in Fig. 2(b). The experimental protocol is summarized in the following:

(1) *Initial-state preparation*. Starting from the equilibrium state, we first initialize the system into the pseudopure state (PPS),

$$\rho_{00} = \frac{1-\delta}{4}\mathbf{1}_4 + \delta|00\rangle\langle 00|,$$

using the line-selective pulses [24], with the polarization $\delta \approx 10^{-5}$. We reconstruct the density matrix of the PPS by quantum state tomography [25,26], and the experimental state

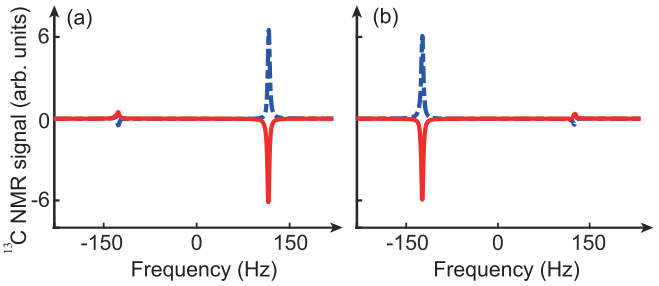

FIG. 3. The experimental ^{13}C spectrum of the final states for (a) $|\epsilon\rangle = |0\rangle$ and (b) $|\epsilon\rangle = |1\rangle$, respectively. The red solid (blue dashed) curve denotes the spectra after the control operation $C_{+U_{\rm id}}$ ($C_{-U_{\rm id}}$).

fidelity,

$$F = \frac{{\rm Tr}\,(\tilde{\rho}_{00}\rho_{\rm th})}{\sqrt{{\rm Tr}[(\tilde{\rho}_{00})^2]\,{\rm Tr}\,(\rho_{\rm th}^2)}} \approx 0.99,$$

where $\rho_{\rm th} = |00\rangle\langle 00|$ and $\tilde{\rho}_{00}$ are the theoretical and experimental density matrix, respectively. Then we can prepare the system spin into the state $|\epsilon\rangle$ with single spin rotations. Finally, a pseudo-Hadamard gate $R_{1y}(\frac{\pi}{2})$ was applied on the first spin to create the target state $\frac{1}{\sqrt{2}}(|0\rangle+|1\rangle)\otimes|\epsilon\rangle$.

(2) *The controlled operation*. The controlled operation $C_{\pm U_{\rm id}}$ (7) is the core of this quantum circuit, which can be realized through the following pulse sequence:

$$R_{2y}\Big(\frac{\alpha^{\pm}}{2}\Big) - R_{2x}\Big(-\frac{\pi}{2}\Big) - e^{-i\alpha^{\pm}I_{1z}I_{2z}} - R_{2x}\Big(\frac{\pi}{2}\Big). \tag{11}$$

Here the evolution under the coupling term $I_{1z}I_{2z}$ is easily realized via the rf pulses and J-coupling evolutions under NMR pulse techniques [4,27], i.e.,

$$\begin{aligned} e^{-i\alpha^{+}I_{1z}I_{2z}} &: \quad e^{-iH_{\rm nmr}\tau^{+}}, \\ e^{-i\alpha^{-}I_{1z}I_{2z}} &: \quad R_{1y}(-\pi) - e^{-iH_{\rm nmr}\tau^{-}} - R_{1y}(\pi), \end{aligned} \tag{12}$$

where $\tau^{\pm} = |\alpha^{\pm}|/(2\pi J)$. The global phase is now encoded in the relative phases of the whole system.

(3) *Measurement*. In NMR, quadrature detection serves as a phase detector, and the encoded global phases of operations (now the relative phases of the whole system) can be extracted via measuring the signal of the ancilla qubit (spin) [1–3]. Taking the state immediately after step (1) as the reference spectrum, we measure the relative phase information by the phase of the Fourier-transformed spectrum. For simplicity, here we choose $|\epsilon\rangle = |0\rangle, |1\rangle$ as the initial state, respectively. In both cases, the spectrum of $|\psi_b^{+}\rangle$ ($|\psi_b^{-}\rangle$) would be a positive (negative) absorption peak, i.e., the phase of the peak is 0 (π). This "inversion of the peak" pattern would be a clear signature for the detection of the global phase. The amplitude and phase of the peaks are obtained by fitting the measured spectrum with complex Lorentzian curves. The global phase ϕ (of operation $-U_{\rm id}$) can be obtained via the difference between phases of the peaks, i.e., $\phi = \pi - 0 = \pi$.

Experimental results. The global phase information can be obtained from the experimental spectra, as displayed in Fig. 3. The result clearly shows the inversion of the peak pattern, indicating the detection of the global phase. For the state

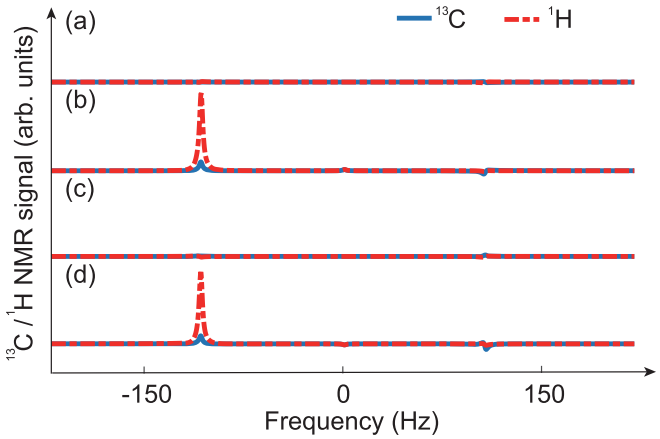

FIG. 4. Experimental ^{13}C and ^{1}H spectra after the implementation of the controlled operations on the states, namely, (a) $C_{+U_{\rm id}}|00\rangle$, (b) $C_{+U_{\rm id}}|10\rangle$, (c) $C_{-U_{\rm id}}|00\rangle$, and (d) $C_{-U_{\rm id}}|10\rangle$, respectively.

$|\epsilon\rangle = |0\rangle$, the phase of the spectrum after the operations $C_{+U_{\rm id}}$ ($C_{-U_{\rm id}}$) are applied is fitted to be 0.02π (0.99π). Then, the global phase (of $-U_{\rm id}$) is evaluated to be 0.97π. For the state $|\epsilon\rangle = |1\rangle$, following the same procedure, the global phase is calculated to be 1.01π. The average global phase is $\overline{\phi} = 0.99\pi$, i.e., with an error of 1% compared to the theoretical value. The global phase difference between the two operations is thus verified. In addition, according to (11), $\pm U_{\rm id}$ should be implemented on the system spin only when the ancilla spin is in state $|1\rangle$. Figure 4 displays the ^{13}C and ^{1}H spectra in experiment after the controlled operations $C_{\pm U_{\rm id}}$ are applied on the initial states $|00\rangle$ and $|10\rangle$, respectively.

We further perform quantum process tomography [28–32] to verify and characterize the controlled operation $C_{\pm U_{\rm id}}$. A set of 16 initial states is prepared, after which the $C_{\pm U_{\rm id}}$ is applied, and the quantum state tomography is applied to reconstruct the final state corresponding to each initial state. With the information of the 16 final states, the process matrix $\chi_{\pm}$ is determined in the basis set $S = \{II, IX, -iIY, IZ, XI, XX, -iXY, XZ, -iYI, YX, -YY, -iYZ, ZI, ZX, -iZY, ZZ\}$, where $X = 2I_x$, $Y = 2I_y$, $Z = 2I_z$, I is a 2 by 2 identity matrix, and the elements in the set are tensor products of them. Figure 5 shows the experimental and theoretical process matrix. The fidelities [30,31]

$$F_\chi = |{\rm Tr}(\chi_{\rm expt}\chi_{\rm th}^\dagger)|/\sqrt{{\rm Tr}(\chi_{\rm expt}\chi_{\rm expt}^\dagger){\rm Tr}(\chi_{\rm th}\chi_{\rm th}^\dagger)}$$

are about 0.99 for both $C_{+U_{\rm id}}$ and $C_{-U_{\rm id}}$. With the help of an ancillary qubit, we thus conclude that we have successfully constructed two SU(2) operations with different global phases on the system qubit, i.e., $+U_{\rm id}$ and $-U_{\rm id}$. The errors mainly come from the state preparation and measurement.

The experimental optimal times to realize $\pm U_{\rm id}$ are given in the following. From Eq. (11), $\pm U_{\rm id}$ on the second spin (if the first spin is in state $|1\rangle$) is realized by $R_{2y}(\frac{\alpha^\pm}{2})$ followed by $e^{-i(2\pi J)\tau^\pm I_{2y}/2}$. The first operation can be realized by a pulse with strength $\omega_{\rm max}$ and duration $|\alpha^\pm|/(2\omega_{\rm max})$, and the second one can be seen as realized by a "pulse" with strength $2\pi J$ and

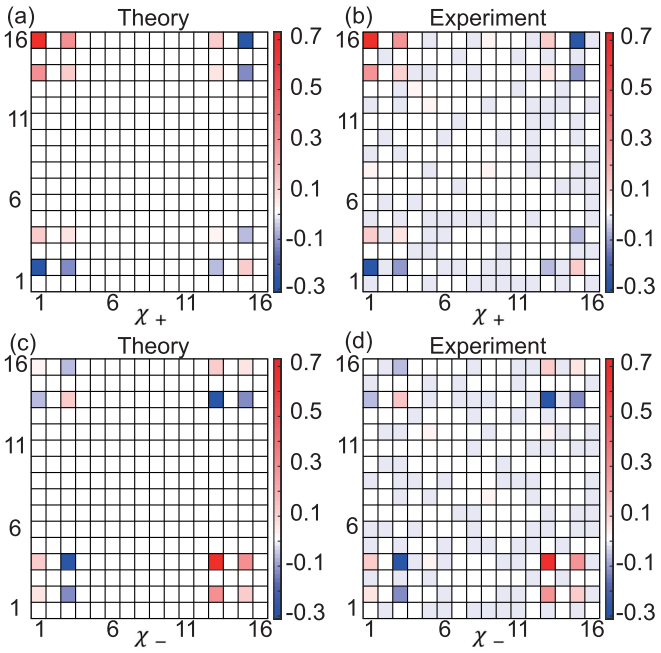

FIG. 5. Theoretical and experimental process matrix (real part) χ_+ of $C_{+U_{\rm id}}$ and χ_- of $C_{-U_{\rm id}}$. The numbers 1 to 16 in the horizontal and vertical axes refer to the operators in the operator basis set S. $|{\rm Imag}(\chi_\pm)| = 0$ in theory, and $|{\rm Imag}(\chi_\pm)| < 0.025$ in the actual experiment.

duration $\tau^\pm/2$. The total operation on the second spin is thus effectively seen as a pulse with strength $\tilde{\omega}_{\rm max}$ and duration $\tilde{T}^\pm$,

$$\tilde{\omega}_{\rm max} = \frac{8\omega_{\rm max}\pi J}{2\omega_{\rm max} + 4\pi J}, \tag{13}$$

$$\tilde{T}^\pm = \frac{|\alpha^\pm|}{2\omega_{\rm max}} + \frac{|\alpha^\pm|}{4\pi J} = \frac{|\alpha^\pm|}{\tilde{\omega}_{\rm max}}, \tag{14}$$

which is just the TOC on the second spin realizing $\pm U_{\rm id}$, with maximum control field strength $\tilde{\omega}_{\rm max}$ and optimal time $\tilde{T}^\pm$. The experimental values are $\tilde{T}^+ = 587.2$ μs, $\tilde{T}^- = 1761.6$ μs, and $\tilde{T}^+/\tilde{T}^- = 1/3$, consistent with the theoretical prediction given in Sec. III.

V. CONCLUSION

In summary, we have experimentally observed the global phase of unitary operations in SU(2), and verified the effect that the global phase has on the optimal time of unitary operations using the NMR technique. Combined with existing theoretical work [11], the physical effect that the global phase has on unitary operations is clarified.

Note that here we study the global phase of unitary operations, not the geometric phase (e.g., [2,3]) of the quantum state of a system. The global phase of an evolution operator manifests itself as the topological phase, which is acquired after a cyclic evolution of maximally entangled qudit pairs under local SU(d) operations [3,4]. As the readout of the global phase of evolution operators requires an auxiliary spin, one may argue that such phases only arise when another spin comes into play. By combining with the previous results that

they also affect the optimal time of unitary operations, we conclude that the global phase we observed indeed belongs to a unitary operation acting upon a one-spin system.

The relation between the optimal time and global phase is also explored theoretically in systems with higher dimension, e.g., a spin-1 system with dimension 3 [14]. To experimentally study the global phases in such systems, one could introduce an ancilla qubit which is coupled to the system and apply the same procedure as given in Sec. III and Fig. 1. For spin-1 systems, a chloroform-D sample could be used where the ^{2}H serves as the system and the ^{13}C serves as the ancilla. The controlled operation on ^{2}H could be implemented utilizing the coupling between ^{13}C and ^{2}H. The global phase information is subsequently read out via the ^{13}C NMR signal. An experiment with spin-1 systems is currently underway as our next work and will be described elsewhere. The results of this paper, together with other related work, have potential impacts on quantum gate designing in quantum information science, and pulse optimization in magnetic resonance spectroscopy [17,18].

ACKNOWLEDGMENTS

Support came from the National Key Research and Development Program of China (Grant No. 2018YFA0306600), National Natural Science Foundation of China (Grants No. 11425523, No. 11661161018, and No. 11847016), Anhui Initiative in Quantum Information Technologies (Grant No. AHY050000), and Scientific Research Plan Projects of Shaanxi Education Department (Grant No. 19JK0132).

[1] D. Suter, K. T. Mueller, and A. Pines, Phys. Rev. Lett. **60**, 1218 (1988).
[2] X. Peng, S. Wu, J. Li, D. Suter, and J. Du, Phys. Rev. Lett. **105**, 240405 (2010).
[3] A. Z. Khoury, A. M. Souza, L. E. Oxman, I. Roditi, R. S. Sarthour, and I. S. Oliveira, Phys. Rev. A **97**, 042343 (2018).
[4] J. Du, J. Zhu, M. Shi, X. Peng, and D. Suter, Phys. Rev. A **76**, 042121 (2007).
[5] A. A. Matoso, X. Sanchez-Lozano, W. M. Pimenta, P. Machado, B. Marques, F. Sciarrino, L. E. Oxman, A. Z. Khoury, and S. Padua, Phys. Rev. A **94**, 052305 (2016).
[6] M. P. Silverman, Eur. J. Phys. **1**, 116 (1980).
[7] J. Du, P. Zou, M. Shi, L. C. Kwek, J. W. Pan, C. H. Oh, A. Ekert, D. K. L. Oi, and M. Ericsson, Phys. Rev. Lett. **91**, 100403 (2003).
[8] Y. Aharonov and L. Susskind, Phys. Rev. **158**, 1237 (1967).
[9] S. A. Werner, R. Colella, A. W. Overhauser, and C. F. Eagen, Phys. Rev. Lett. **35**, 1053 (1975).
[10] M. E. Stoll, A. J. Vega, and R. W. Vaughan, Phys. Rev. A **16**, 1521 (1977).
[11] S. J. Glaser, U. Boscain, T. Calarco, C. P. Koch, W. Kockenberger, R. Kosloff, I. Kuprov, B. Luy, S. Schirmer, T. Schulte-Herbruggen, D. Sugny, and F. K. Wilhelm, Eur. Phys. J. D **69**, 279 (2015).
[12] A. Garon, S. J. Glaser, and D. Sugny, Phys. Rev. A **88**, 043422 (2013).
[13] T. Schulte-Herbruggen, A. Sporl, N. Khaneja, and S. J. Glaser, Phys. Rev. A **72**, 042331 (2005).
[14] V. P. Shauro and V. E. Zobov, Phys. Rev. A **88**, 042320 (2013).
[15] V. P. Shauro, Quantum Inf. Proc. **14**, 2345 (2015).
[16] K. W. Moore Tibbetts, C. Brif, M. D. Grace, A. Donovan, D. L. Hocker, T. S. Ho, R. B. Wu, and H. Rabitz, Phys. Rev. A **86**, 062309 (2012).
[17] M. A. Janich, R. F. Schulte, M. Schwaiger, and S. J. Glaser, J. Magn. Reson. **213**, 126 (2011).
[18] K. Kobzar, S. Ehni, T. E. Skinner, S. J. Glaser, and B. Luy, J. Magn. Reson. **225**, 142 (2012).
[19] J. F. Cornwell, *Group Theory in Physics: An Introduction* (Academic, San Diego, 1997).
[20] U. Dorner, R. Demkowicz-Dobrzanski, B. J. Smith, J. S. Lundeen, W. Wasilewski, K. Banaszek, and I. A. Walmsley, Phys. Rev. Lett. **102**, 040403 (2009).
[21] T. Denkmayr, H. Geppert, H. Lemmel, M. Waegell, J. Dressel, Y. Hasegawa, and S. Sponar, Phys. Rev. Lett. **118**, 010402 (2017).
[22] F. A. Vind, A. Foerster, I. S. Oliveira, R. S. Sarthour, D. D. O. Soares-Pinto, A. M. D. Souza, and I. Roditi, Sci. Rep. **6**, 20789 (2016).
[23] R. S. Said, D. W. Berry, and J. Twamley, Phys. Rev. B **83**, 125410 (2011).
[24] X. Peng, X. Zhu, X. Fang, M. Feng, K. Gao, X. Yang, and M. Liu, Chem. Phys. Lett. **340**, 509 (2001).
[25] J.-S. Lee, Phys. Lett. A **305**, 349 (2002).
[26] Y. Ji, J. Bian, X. Chen, J. Li, X. Nie, H. Zhou, and X. Peng, Phys. Rev. A **99**, 032323 (2019).
[27] L. M. K. Vandersypen and I. L. Chuang, Rev. Mod. Phys. **76**, 1037 (2005).
[28] M. A. Nielsen and I. L. Chunag, *Quantum Computation and Quantum Information* (Cambridge University Press, Cambridge, 2015).
[29] J. Geng, Y. Wu, X. Wang, K. Xu, F. Shi, Y. Xie, X. Rong, and J. Du, Phys. Rev. Lett. **117**, 170501 (2016).
[30] G. Feng, G. Xu, and G. Long, Phys. Rev. Lett. **110**, 190501 (2013).
[31] J. Zhang, A. M. Souza, F. D. Brandao, and D. Suter, Phys. Rev. Lett. **112**, 050502 (2014).
[32] Y. S. Weinstein, T. F. Havel, J. Emerson, N. Boulant, M. Saraceno, S. Lloyd, and D. G. Cory, J. Chem. Phys. **121**, 6117 (2004).